Arabian Journal of Geosciences (2019) 12: 452
https://doi.org/10.1007/s12517-019-4628-1

ORIGINAL PAPER

The compressive-shear fracture strength of rock containing water based on Druker-Prager failure criterion

Yanlin Zhao[1,2] • Yixian Wang[3] • Liming Tang[1]

Received: 7 January 2019 / Accepted: 10 July 2019 / Published online: 22 July 2019

Abstract

The stresses at the tips of the compressive-sheared cracks were calculated by applying the superposition principle. Then, the principal stresses at the tips of the compressive-shear crack were obtained. According to the Druker-Prager criterion, a fracture criterion for the compressive-shear crack, verified reasonable, was proposed. In addition, considering the influence of water, the above criterion was modified to investigate the influence of water on the stress intensity factors of cracks. The results show that the third principal stress of the main crack surface significantly increases the rock strength when the internal friction angle of the rock is lower than crack inclination angle. However, when the internal friction angle is higher than crack inclination angle, the increase of water pressure dramatically decreases the rock strength. When the internal friction angle is equal to crack inclination angle, the influences of water pressure and the third principal stress on the rock strength are the same. In addition, when crack inclination angle is lower than 30°, the third principal stress greatly influences the rock strength.

Keywords Water action · The Drucker-Prager criterion · Stress intensity factor · Crack · Fracture strength

Introduction

Rocks are complex geological masses, containing extensive joints and fissures, because of the formation complexity. In addition, water frequently affects the underground rocks. Therefore, the mechanical properties of rocks, including the anisotropy, the heterogeneity, and the variation of strength resulting from the water-rock interaction, are complicated (Zhao et al. 2017a; Liste and Kerr 1991).

Many experimental and theoretical studies have investigated the influence of crevice and pore water pressure on rock/soil strength (Zhao et al. 2019; Wang et al. 2017; 2018, 2019a). Bidgoli and Jing (2015) used discrete element methods to simulate the rheological process of the fractured rock mass, and they found that water pressure has significant influence on the strength. Wong et al. (2015) studied the effects of water on rock strength, porosity, density, fabric of rocks, and external factors. Based on the rock fracture mechanics criterion, Liu et al. (2014) established a damage fracture mechanical model for the rock mass in the compression-shear state. Zhao et al. (2018) considered the penetration mechanism of cracked rock cracks under seepage pressure and proposed a corresponding failure criterion. Wei et al. (2018) developed a further improved maximum tangential stress criterion for estimating tensile fracture strength of cracked rock, and laboratory tests show that the criterion can predict experimental results well. Considering the actual effect of the water pressure on the stress field at crack tips, Tang et al. (2004) proposed a new criterion for the fracture strength of fractured rock under water.

The initiation, propagation, and coalescence of the internal defects, such as cracks, may lead to the deformation and the failure of rocks (Wei et al. 2015; Xu et al. 2016; Dai et al. 2016). Therefore, researchers have proposed extensive fracture criteria, using the fracture mechanics and the failure criterion for rock (Wei et al. 2017). For instance, Liu et al. (2004) investigated the relation between the Druker-Prager failure

Editorial handling: Murat Karakus

✉ Yixian Wang
Wangyixian2012@hfut.edu.cn

Yanlin Zhao
Yanlin_8@163.com

1 Hunan Provincial Key Laboratory of Safe Mining Techniques of Coal Mines, Work Safety Key Lab on Prevention and Control of Gas and Roof Disasters for Southern Coal Mines, Hunan University of Science and Technology, Xiangtan, Hunan, China

2 State Key Laboratory of Coal Resources and Safety Mining, China University of Mining and Technology, Xuzhou, Jiangsu, China

3 Hefei University of Technology, Hefei, Anhui, China

criterion and the fracture toughness (K_I and K_{II}) by substituting the total stresses at crack tips into the Druker-Prager failure criterion. Gao et al. (2017) proposed a new fracture criterion based on the energy principles, then, they studied the crack propagation process using this criterion. Zhou et al. (2007) established the criterion for compression-shear fracture using some failure criteria for geomaterials. Zuo et al. (2008) developed a nonlinear strength criterion for rock-like materials, then, they investigated the relation between the flaw inclination and the axial load. In addition, some researchers determine the peak strength of rock by introducing the GSI, which provides a basis for rock failure (Xuan and Zhang 2016; Jiang et al. 2018; Chu and Ji 2017). The above studies indicate that it is feasible to establish new fracture criteria, based on the macroscopic failure criterion.

The current studies have significantly contributed to understanding the fracture characteristics, and make the rock have a certain early warning before the fracture (Dai et al. 2015; Wei et al. 2016). However, few studies have incorporated the fracture theory and the macroscopic failure criteria to investigate the effect of the water on rock fracture strength, meanwhile, few analysis and summary, the influence of crack inclination angle and the internal friction angle on rock strength under the water-force action of rock compression and shear, has been done. Considering the effect of water on the stress intensity factors, this paper proposed a newly rock fracture criterion considering the influence of water by applying the Druker-Prager failure criterion and the fracture theory.

The stress intensity factors at crack tips considering the influence of water

The rock strength may be decreased by water pressure and hydro-chemical damage (Zhao et al. 2017b, c; Wang et al. 2019). Figure 1 shows the biaxial stress state of the rock, considering the influences of crack and water.

According to Fig. 1, the normal stress applied on the main crack surface σ and the shear stress applied on the main crack surface τ can be obtained (Guo et al. 2002). In this paper, the compressive stress is positive.

$$\left.\begin{aligned}\sigma &= \frac{1}{2}[(\sigma_1+\sigma_3)+(\sigma_1-\sigma_3)\cos 2\beta]-P\\ \tau &= \frac{1}{2}(\sigma_1-\sigma_3)\sin 2\beta\end{aligned}\right\} \tag{1}$$

where σ_1 and σ_3 are the first and the third principal stresses of the main crack surface, respectively. β is the crack inclination angle; P is the water pressure, acting on the crack surface.

In the fracture mechanics, cracks are often classified into three types according to their forces and crack propagation paths. These cracks are the opening crack (the mode I crack),

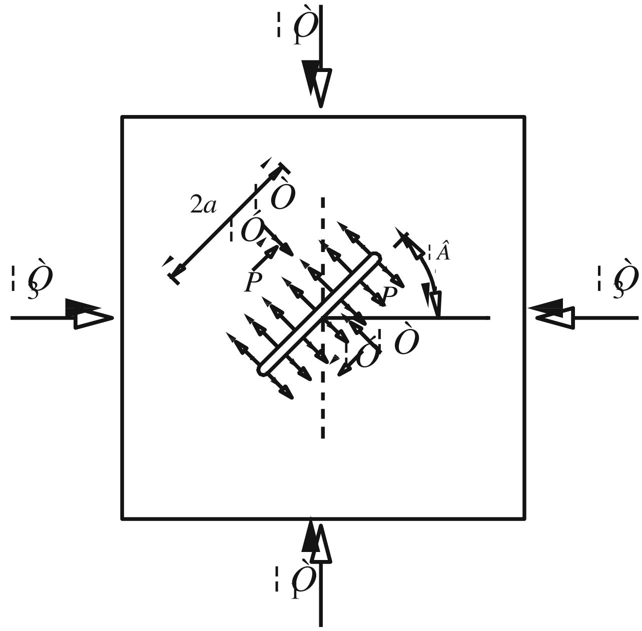

Fig. 1 The biaxial stress state of the cracked rock influenced by water

the sliding mode crack (the mode II crack), and the tearing mode crack (the mode III crack). The three-mode cracks are shown in Fig. 2.

For the mode I crack:

$$K_I = \sigma\sqrt{\pi a} \tag{2}$$

where K_I is the stress intensity factor of mode I crack; π is a constant and a is the half-length of the crack.

Considering the influence of water, the stress intensity factor is:

$$K_I = \left\{\frac{1}{2}[(\sigma_1+\sigma_3)+(\sigma_1-\sigma_3)\cos 2\beta]-P\right\}\sqrt{\pi a} \tag{3}$$

For the mode II crack:

$$K_{II} = \tau\sqrt{\pi a} \tag{4}$$

where K_{II} is the stress intensity factor of mode II crack.

First, when the crack is open, the stress intensity factor of the mode II crack, influenced by water (the state of stress has been shown in Fig. 3), is:

$$K_{II} = \frac{1}{2}(\sigma_1-\sigma_3)\sin 2\beta\sqrt{\pi a} \tag{5}$$

Second, when the crack is fully closed, the stress intensity factor of the mode II crack, influenced by water, is:

$$K_{II} = \frac{1}{2}(\sigma_1-\sigma_3)\sin 2\beta\sqrt{\pi a}-(c+\sigma\tan\varphi)\sqrt{\pi a} \tag{6}$$

where c and φ are the cohesion and the internal friction angle of the rock, respectively.

Fig. 2 The three-mode cracks

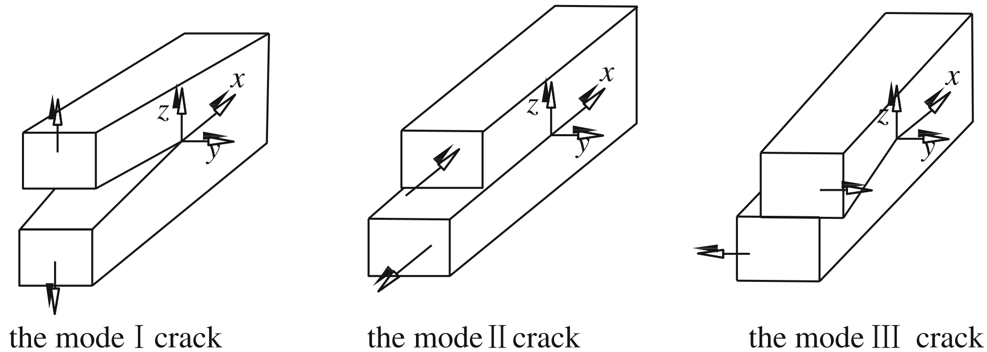

The stress field at rock crack tips in the compressive-shear state

Figure 4 shows the stress and the strain fields at a certain point A near the crack tip. To facilitate the calculation the stress, we transformed the calculation system (Fig. 5):

Using the superposition criterion, the stress field at the tip of the mode I–II cracks is (Yu et al. 1991):

$$\left.\begin{aligned}\sigma_x &= \frac{K_I}{\sqrt{2\pi r}}\cos\frac{\theta}{2}\left(1-\sin\frac{\theta}{2}\sin\frac{3}{2}\theta\right)-\frac{K_{II}}{\sqrt{2\pi r}}\sin\frac{\theta}{2}\left(2+\cos\frac{\theta}{2}\cos\frac{3}{2}\theta\right)\\ \sigma_y &= \frac{K_I}{\sqrt{2\pi r}}\cos\frac{\theta}{2}\left(1+\sin\frac{\theta}{2}\sin\frac{3}{2}\theta\right)+\frac{K_{II}}{\sqrt{2\pi r}}\sin\frac{\theta}{2}\cos\frac{\theta}{2}\cos\frac{3}{2}\theta\\ \tau_{xy} &= \frac{K_I}{\sqrt{2\pi r}}\sin\frac{\theta}{2}\cos\frac{\theta}{2}\cos\frac{3}{2}\theta+\frac{K_{II}}{\sqrt{2\pi r}}\cos\frac{\theta}{2}\left(1-\sin\frac{\theta}{2}\sin\frac{3}{2}\theta\right)\end{aligned}\right\} \quad (7)$$

where θ and r are the angle and the distance between a certain point A near the crack tip and the polar axis, respectively.

Under the plane stress condition, σ_2 is equal to 0; therefore, the principal stresses are:

$$\left.\begin{aligned}\sigma_1 &= \frac{\sigma_x+\sigma_y}{2}+\sqrt{\left(\frac{\sigma_x-\sigma_y}{2}\right)^2+\tau_{xy}{}^2}\\ \sigma_3 &= \frac{\sigma_x+\sigma_y}{2}-\sqrt{\left(\frac{\sigma_x-\sigma_y}{2}\right)^2+\tau_{xy}{}^2}\end{aligned}\right\} \quad (8)$$

Equations (7) and (8) yield the principle stresses at the tips of the crack in the compressive-shear state (Yu et al. 1991):

$$\left.\begin{aligned}\sigma_1 &= \frac{1}{\sqrt{2\pi r}}(K_a+K_b)\\ \sigma_3 &= \frac{1}{\sqrt{2\pi r}}(K_a-K_b)\end{aligned}\right\} \quad (9)$$

$$\text{where}\ \begin{cases} K_a = K_I\cos\frac{\theta}{2}-K_{II}\sin\frac{\theta}{2}\\ K_b = \frac{1}{2}\sqrt{(K_I\sin\theta+2K_{II}\cos\theta)^2+K_{II}{}^2\sin^2\theta}\end{cases}$$

The D-P failure criterion

Extensive failure criteria, including the Griffith criterion, the modified Griffith criterion, the Druker-Prager failure criterion, the Coulomb-Mohr criterion, the Hoek-Brown criterion, and

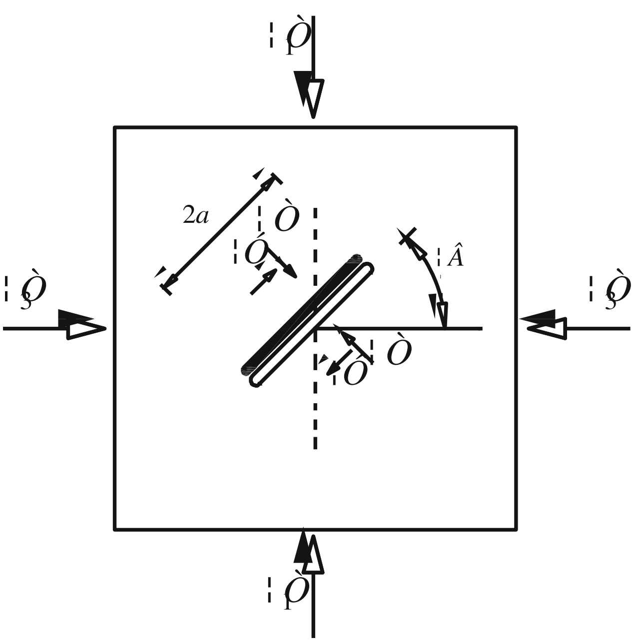

Fig. 3 The force state of fully closed crack

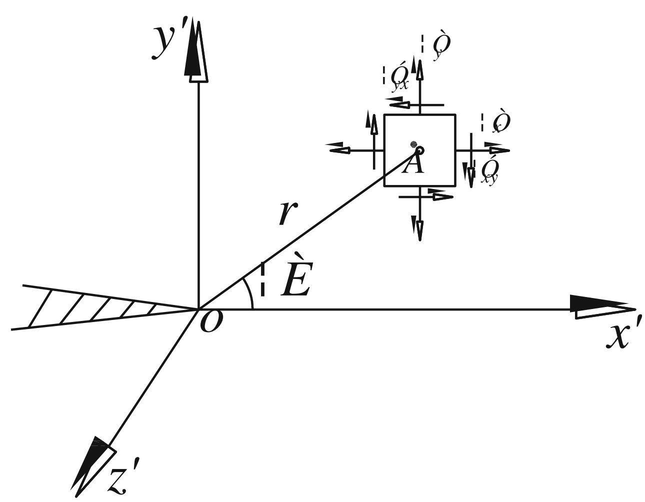

Fig. 4 The stress and the strain field at a certain point A near the crack tip

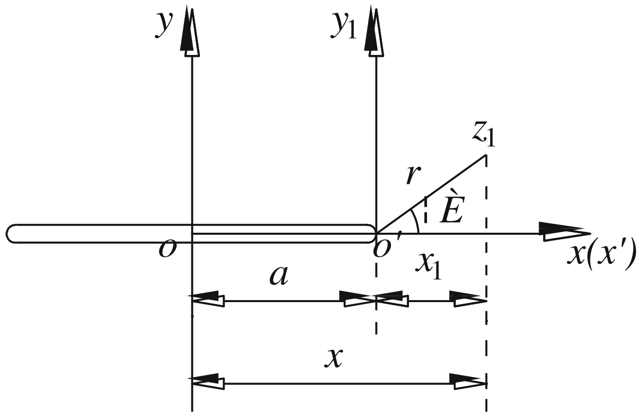

Fig. 5 New and old coordinate systems with the center and the top of the crack as the origin of the coordinate, respectively

the Mises criterion, have been proposed. However, researchers failed to propose a universal criterion to predict the rock properties (Wu et al. 2019; Yang et al. 2008; Liu et al. 2017; Zhao et al. 2016; Wang et al. 2014), because of the various application conditions for the above criteria.

In 1952, Drucker and Prager proposed a failure criterion, based on the modification and development of the Mises criterion. By introducing the first stress invariant into the Mises criterion, this criterion is written as:

$$f(I_1, J_2) = \alpha I_1 + \sqrt{J_2} - k = 0 \tag{10}$$

where I_1 is the first invariants of the stress tensor,

$$I_1 = \sigma_1 + \sigma_2 + \sigma_3 \tag{11}$$

J_2 is the second invariants of the stress deviator:

$$J_2 = \frac{1}{6}\left[(\sigma_1 - \sigma_2)^2 + (\sigma_2 - \sigma_3)^2 + (\sigma_3 - \sigma_1)^2\right] \tag{12}$$

α and k are constants which are written as:

$$\begin{cases} \alpha = \dfrac{2\sin\varphi}{\sqrt{3}(3 - \sin\varphi)} \\ k = \dfrac{6c\cos\varphi}{\sqrt{3}(3 - \sin\varphi)} \end{cases}$$

The criterion for the compressive-shear fracture based on the Druker-Prager failure criterion

The criterion for the compressive-shear fracture

Based on the maximum tensile stress fracture criterion (Erdogan and Sih 1963), the initiation angles (θ_0) of the central oblique crack in compressive-shear states are equal to 0 and 70.5° for the mode I crack and the mode II crack, respectively.

Equations (9), (11), and (12) yield:

$$I_1 = \frac{2}{\sqrt{2\pi r}} K_\mathrm{a} \tag{13}$$

$$J_2 = \frac{1}{6\pi r}\left(3{K_\mathrm{b}}^2 + {K_\mathrm{a}}^2\right) \tag{14}$$

By substituting Eqs. (13) and (14) into Eq. (10), the compressive-shear fracture criterion can be written as:

$$\alpha \frac{2}{\sqrt{2\pi r}} K_\mathrm{a} + \frac{1}{\sqrt{6\pi r}} \sqrt{3{K_\mathrm{b}}^2 + {K_\mathrm{a}}^2} - k = 0 \tag{15}$$

For the pure mode I crack with the θ_0 of 0, K_a and K_b are equal to K_I and 0, respectively. Then, Eq. (15) yields:

$$\frac{2\alpha K_I}{\sqrt{2\pi r}} + \frac{K_I}{\sqrt{6\pi r}} = k \tag{16}$$

When the stress intensity reaches the fracture toughness, then it yields:

$$K_{IC} = \frac{k\sqrt{6\pi r}}{2\sqrt{3}\alpha + 1} \tag{17}$$

By substituting Eq. (17) into Eq. (15), the criterion is written as:

$$\frac{2\alpha K_\mathrm{a}\sqrt{3} + \sqrt{3{K_\mathrm{b}}^2 + {K_\mathrm{a}}^2}}{\left(2\sqrt{3}\alpha + 1\right)K_\mathrm{IC}} - 1 = 0 \tag{18}$$

Feasibility verification of the criterion without the influence of the water

To verify the feasibility of the proposed criterion, we compared the results of this criterion with those from the maximum-tangential-stress theory. The special cases for the maximum tangential stress theory are:

First, for the mode I crack, K_{II} and θ_0 are equal to 0. Therefore, K_I is equal to K_{IC}.

Additionally, for the mode II crack, K_I and θ_0 are equal to 0 and − 70.5°, respectively. Therefore, according to the maximum tensile stress criterion (Liu et al. 2017), when the material parameter of the rock, Poisson's ratio ν is equal to 0, then, K_{IIC} is equal to 0.866 K_{IC}.

For the proposed criterion, Eq. (18) yields:

For the mode I crack, K_{II} and θ_0 are equal to 0. Thus, the fracture toughness in Eq. (17) is equal to K_I.

For the mode II crack, K_I and θ_0 are equal to 0 and − 70.5°, respectively. The fracture toughness in Eq. (15) is:

$$K_\mathrm{IIC} = \frac{k\sqrt{\pi r}}{0.4715 + 0.8161\alpha} \tag{19}$$

Based on Eqs. (17) and (19), we can obtain that:

$$\frac{K_{IIC}}{K_{IC}}=\frac{2\sqrt{3}\alpha+1}{\sqrt{6}(0.4715+0.8161\alpha)} \tag{20}$$

where α determines $\frac{K_{IIC}}{K_{IC}}$. In addition, when φ and α are equal to 0, $\frac{K_{IIC}}{K_{IC}}$ is equal to 0.866, the same value to that of the maximum-tangential-stress theory. Thus, this criterion based on the Druker-Prager failure criterion is reasonable.

The criterion of the compressive-shear fracture considering water action

Extensive studies (Zhao et al. 2017d; Huang et al. 2017; Wang et al. 2019b, c) have investigated the strength and the failure mode of the crack in compressive-shear state. However, the strength of the rock, subjected to the compressive-shear stress and the water action, lacks detailed investigations (Zhang et al. 2011; Zhao et al. 2017e). Thus, based on the above criterion in the compressive-shear state, this paper proposed a strength criterion by introducing the stress intensity factors of the mode I crack and the mode II crack, subjected to the compressive-shear stress and the water action. According to the failure forms of the rock, containing a crack, the following three conditions are considered:

For the closed crack, the maximum values of the stress intensity factor of the mode I crack and the mode II crack are equal to 0 (Guo et al. 2002). The above results show that when the crack propagates in a tensile manner, K_{II} is equal to 0. However, K_I is equal to 0 when the crack propagates in a shear manner, in other words, cracks propagate on the plane of the main crack.

For the mode I crack propagation, K_{II} is equal to 0, Eq. (18) yields:

$$K_I=\frac{(2\sqrt{3}\alpha+1)K_{IC}}{2\sqrt{3}\alpha\cos\frac{\theta}{2}+\sqrt{\frac{3}{4}\sin^2\theta+\cos^2\frac{\theta}{2}}} \tag{21}$$

By substituting Eq. (21) into Eq. (3), the initiation criterion influenced by water is:

$$\sigma_1=\frac{2P}{1+\cos2\beta}+\frac{(\cos2\beta-1)\sigma_3}{1+\cos2\beta}+\frac{2(2\sqrt{3}\alpha+1)K_{IC}}{\left(2\sqrt{3}\alpha\cos\frac{\theta}{2}+\sqrt{\frac{3}{4}\sin^2\theta+\cos^2\frac{\theta}{2}}\right)}\frac{1}{(1+\cos2\beta)\sqrt{\pi a}} \tag{22}$$

Under certain conditions, the variables, excluding t σ_1 and P, are known. σ_1 linearly increases with the increase of P.

To express the relationship of σ_1 and P, we supposed $m_1=\frac{2}{1+\cos2\beta}$, $n_1=\frac{(\cos2\beta-1)}{1+\cos2\beta}$, $t_1=\frac{2(2\sqrt{3}\alpha+1)K_{IC}}{\left(2\sqrt{3}\alpha\cos\frac{\theta}{2}+\sqrt{\frac{3}{4}\sin^2\theta+\cos^2\frac{\theta}{2}}\right)}\frac{1}{(1+\cos2\beta)\sqrt{\pi a}}$,

Then, Eq. (22) can be written as:

$$\sigma_1=m_1P+n_1\sigma_3+t_1 \tag{23}$$

Under certain conditions, Eq. (23) shows that the variables, except σ_3, P, and β, are known, β directly determines the effect of P on σ_1. Obviously, $|\frac{m_1}{n_1}|$ and m_1 increase with the increase of β. This indicates that P plays a leading role on the rock strength, and when β increases, the rock strength will be significantly promoted.

This phenomenon is reasonable because the water pressure leads to the decreases in the effective stress on the crack surfaces and K_I. Then, the delay of the crack initiation, resulting from the decrease in K_I, the initiation strength of rock blocks, is increased.

For the mode II crack propagation, K_I is equal to 0, Eq. (18) yields:

$$K_{II}=\frac{(2\sqrt{3}\alpha+1)K_{IC}}{\sqrt{\frac{3}{4}+\frac{9}{4}\cos^2\theta+\sin^2\frac{\theta}{2}-2\sqrt{3}\alpha\sin\frac{\theta}{2}}} \tag{24}$$

By substituting Eq. (24) into Eq. (6), the crack rock initiation strength criterion, considering water action, is:

$$\sigma_1=\frac{[\sin2\beta+(1-\cos2\beta)\tan\varphi]\sigma_3-2\tan\varphi P}{\sin2\beta-(1+\cos2\beta)\tan\varphi}+\frac{-2c}{\sin2\beta-(1+\cos2\beta)\tan\varphi}+\frac{2(2\sqrt{3}\alpha+1)K_{IC}}{[\sin2\beta-(1+\cos2\beta)\tan\varphi]\left(\sqrt{\frac{3}{4}+\frac{9}{4}\cos^2\theta+\sin^2\frac{\theta}{2}-2\sqrt{3}\alpha\sin\frac{\theta}{2}}\right)\sqrt{\pi a}} \tag{25}$$

In order to express the relationship of σ_1 and P, suppose $m_2=\frac{-2\tan\varphi}{\sin2\beta-(1+\cos2\beta)\tan\varphi}$, $n_2=\frac{\sin2\beta+(1-\cos2\beta)\tan\varphi}{\sin2\beta-(1+\cos2\beta)\tan\varphi}$, $t_2=\frac{-2c}{\sin2\beta-(1+\cos2\beta)\tan\varphi}+\frac{2(2\sqrt{3}\alpha+1)K_{IC}}{[\sin2\beta-(1+\cos2\beta)\tan\varphi]\left(\sqrt{\frac{3}{4}+\frac{9}{4}\cos^2\theta+\sin^2\frac{\theta}{2}-2\sqrt{3}\alpha\sin\frac{\theta}{2}}\right)\sqrt{\pi a}}$ then Eq.(25) can be written as:

$$\sigma_1=m_2P+n_2\sigma_3+t_2 \tag{26}$$

Obviously, m_2 and n_2 will directly determine the effect of P and σ_3 on σ_1. Moreover, the parameters m_2 and n_2 are related with β and φ. Therefore, we considered the change of $|\frac{m_2}{n_2}|$ to determine whether P or σ_3 significantly affect the rock strength.

First, when β changes, φ remains unchanged, other parameters are known, and according to the calculation parameters in Table 1, the curve of $|\frac{m_2}{n_2}|$ and β under different φ can be obtained (Fig. 6).

When β increases to φ, $|\frac{m_2}{n_2}|$ sharply decrease from about 9.5, 10.5, and 11 to 1 (Fig. 6). Then these values slightly

Table 1 Calculation parameter

Lithology	Friction angle φ/(°)	Crack inclination angle β/(°)
Red sandstone	35	0~90
Marble	47	
Lherzolitic	53	

decrease to about 0.73, 0.84, and 0.88, respectively. Finally, these values increase to 1 when β increases to 90°.

The above descriptions show that when β is lower than φ, the increase in P can significantly decrease the rock strength. However, when β is higher than φ, the rock strength can be significantly increased by the increase of σ_3 instead of that of P. In addition, when β is lower than φ, greater influence of P on σ_1 is observed by the increase in φ.

Second, when φ varies, β remains unchanged, other parameters are known. According to the calculation parameters in Table 2, we obtained the curve of $|\frac{m_2}{n_2}|$ and φ under different β (Fig. 7).

In this paper, according to the actual situation, the internal friction angle of the rock was 10°~75°.

For the β of 15°, 30°, 45°, 60°, and 75°, Fig. 7 shows that the increase of φ leads to the increase of $|\frac{m_2}{n_2}|$. When the β increases to φ, $|\frac{m_2}{n_2}|$ increases to 1. Particularly, for the β of 90°, $|\frac{m_2}{n_2}|$ is 1.

The above results show that σ_3 significantly increases the rock strength when φ is lower than β. However, when φ is higher than β, the increase of P dramatically decreases the rock strength. When φ is equal to β, the influences of P and σ_3 on σ_1 are the same. In addition, when β is lower than 30° and φ, σ_3 greatly influences σ_1.

For the open crack, the mode I crack propagation occurs instead of the mode II crack propagation. Correspondingly, the maximum stress intensity factor for the mode I crack corresponds to the condition of $K_{II} = 0$. Thus, the crack propagation path is in accordance with the path for the $K_{II} = 0$, and the crack initiation criterion can be presented by Eq. (22).

Table 2 Calculation parameter

Friction angle φ/(°)	Crack inclination angle β/(°)
10~75	15/30/45/60/75/90

Conclusions

(1) Based on the Druker-Prager failure criterion and the theory of fracture mechanics, a newly proposed criterion for the compressive-shear fracture is proven reasonable.
(2) The results show that the water pressure improves the rock strength for the mode I crack, whereas for the mode II crack, the water pressure has a very complicated effect on the rock strength for the closed crack. And the water pressure decreases the rock strength for the open crack.
(3) Moreover, the results show that the third principal stress significantly increases the rock strength when the internal friction angle of the rock is lower than the crack inclination angle. However, when the internal friction angle is higher than the crack inclination angle, the increase of water pressure dramatically decreases the rock strength. When the internal friction angle is equal to crack inclination angle, the influences of water pressure and the third principal stress on the rock strength are the same. In addition, when crack inclination angle is lower than 30°, the third principal stress influences the rock

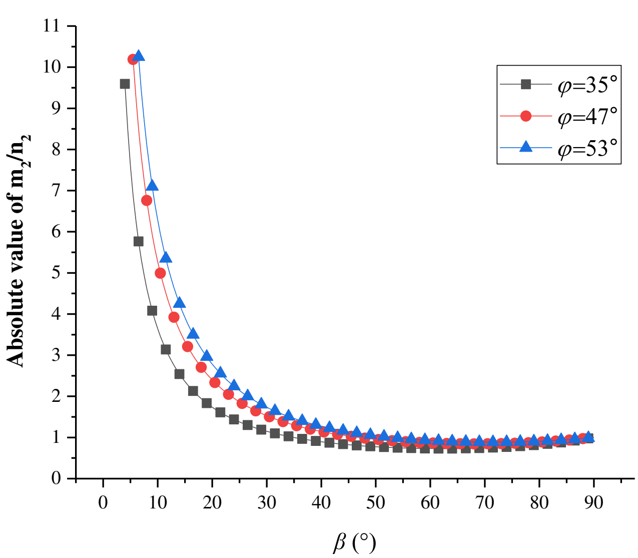

Fig. 6 The curves of $|\frac{m_2}{n_2}|$ versus β under different φ

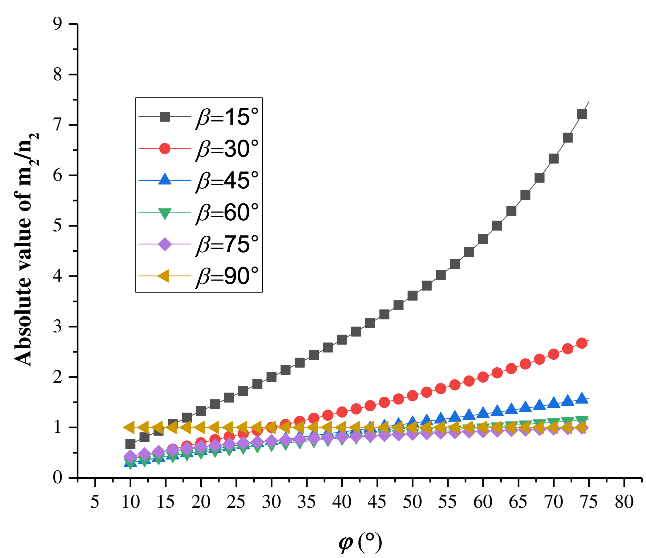

Fig. 7 The curves of $|\frac{m_2}{n_2}|$ versus φ under different β

strength greatly. Generally, the water pressure decreases the rock strength.

Funding information This research is supported by the National Natural Science Foundation of China (51774131, 51774107), the Natural Science Foundation of Hunan province (2015JJ2067), the CRSRI Open Research Program (CKWV2017508/KY), and the Open Projects of State Key Laboratory of Coal Resources and Safe Mining, CUMT (SKLCRSM16KF12).

References

Bidgoli MN, Jing L (2015) Water pressure effects on strength and deformability of fractured rocks under low confining pressures. Rock Mech Rock Eng 48:971–985

Chu CM, Ji YS (2017) Calculation on high rock slope strength parameter based on GSI. J Liaoning Tech Univ (Nat Sci) 36(5):488–493

Dai F, Wei MD, Xu NW, Ma Y, Yang DS (2015) Numerical assessment of the progressive rock fracture mechanism of cracked chevron notched Brazilian disc specimens. Rock Mech Rock Eng 48:463–479

Dai F, Xu Y, Zhao T, Xu NW, Liu Y (2016) Loading-rate-dependent progressive fracturing of cracked chevron-notched Brazilian disc specimens in split Hopkinson pressure bar tests. Int J Rock Mech Min Sci 88:49–60

Erdogan F, Sih GC (1963) On the crack extension in plates under plane loading and transverse shear. J Basic Eng 85(4):519-525

Gao W, Dai S, Xiao T, He TY (2017) Failure process of rock slopes with cracks based on the fracture mechanics method. Eng Geol 231:190–199

Guo SH, Sun ZQ, Xie XQ (2002) Research on mode and criterion of rock fracture under compressive loading. Chin J Geotech Eng 24:304–308

Huang YH, Yang SQ, Ranjith PG, Zhao J (2017) Strength failure behavior and crack evolution mechanism of granite containing pre-existing non-coplanar holes: Experimental study and particle flow modeling. Comput Geotech 88:182–198

Jiang GC, Hu NL, Hong GY, Li GQ, Fang JZ (2018) Determination of rock mass mechanical parameters based on quantification and correction method of GSI value. Rock Soil Mech 39(6):2211–2218 (in Chinese)

Liste JR, Kerr RC (1991) Fluid-mechanical models of crack propagation and their application to magma transport in dykes. J Geophys Res Solid Earth 96:10049–10077

Liu J, Li JL, Zhou JF, Chen PS, Chen XZ (2004) Research on relation of D-P failure criterion and rock fracture toughness K_{Ic}, K_{IIc}. Chin J Rock Mech Eng 23:4300–4302

Liu TY, Cao P, Lin H (2014) Damage and fracture evolution of hydraulic fracturing in compression-shear rock cracks. Theor Appl Fract Mech 74:55–63

Liu T, Lin BQ, Yang W (2017) Mechanical behavior and failure mechanism of pre-cracked specimen under uniaxial compression. Tectonophysics 712–713:330–343

Tang LS, Zhang PC, Wang Y (2004) On fracture strength of rocks with cracks under water action. Chin J Rock Mech Eng 23:3337–3341

Wang SY, Sloan SW, Sheng DC, Yang SQ, Tang CA (2014) Numerical study of failure behaviour of pre-cracked rock specimens under conventional triaxial compression. Int J Solids Struct 51:1132–1148

Wang YX, Guo PP, Ren WX, Yuan BX, Yuan HP, Cao P (2017) Laboratory investigation on strength characteristics of expansive soil treated with jute fiber reinforcement. Int J Geomech 17(11):04017101

Wang YX, Guo PP, Dai F, Li X, Zhao YL, Liu Y (2018) Behavior and modeling of fiber-reinforced clay under triaxial compression by combining the superposition method with the energy-based homogenization technique. Int J Geomech 18(12):04018172

Wang F, Cao P, Cao RH, Xiong XG, Hao J (2019) The influence of temperature and time on water–rock interactions based on the morphology of rock joint surfaces. Bull Eng Geol Environ 78(5):3385-3394

Wang YX, Guo PP, Li X, Lin H (2019a) Behavior of fiber-reinforced and lime-stabilized clayey soil in triaxial tests. Appl Sci-Basel 9(5):900

Wang YX, Shan SB, Zhang CS, Guo PP (2019b) Seismic response of tunnel lining structure in a thick expansive soil stratum. Tunn Undergr Space Technol 88:250–259

Wang YX, Lin H, Zhao YL, Li X, Guo PP, Liu Y (2019c) Analysis of fracturing characteristics of unconfined rock plate under edge on impact loading. Eur J Environ Civ Eng. https://doi.org/10.1080/19648189.2018.1509021

Wei MD, Dai F, Xu NW, Xu Y, Xia K (2015) Three-dimensional numerical evaluation of the progressive fracture mechanism of cracked chevron notched semi-circular bend rock specimens. Eng Fract Mech 134:286–303

Wei MD, Dai F, Xu NW, Zhao T (2016) Stress intensity factors and fracture process zones of ISRM-suggested chevron notched specimens for mode I fracture toughness testing of rocks. Eng Fract Mech 168:174–189

Wei MD, Dai F, Xu NW, Liu Y, Zhao T (2017) Fracture prediction of rocks under mode I and mode II loading using the generalized maximum tangential strain criterion. Eng Fract Mech 186:21–38

Wei MD, Dai F, Zhou JW, Liu Y, Luo J (2018) A further improved maximum tangential stress criterion for assessing mode I fracture of rocks considering non-singular stress terms of the Williams expansion. Rock Mech Rock Eng 51:3471–3488

Wong LNY, Maruvanchery V, Liu G (2015) Water effects on rock strength and stiffness degradation. Acta Geotech 11:1–25

Wu QH, Weng L, Zhao YL, Guo BH, Luo T (2019) On the tensile mechanical characteristics of fine-grained granite after heating/cooling treatments with different cooling rates. Eng Geol 253:94–110. https://doi.org/10.1016/j.enggeo.2019.03.014

Xu Y, Dai F, Xu NW, Zhao T (2016) Numerical investigation of dynamic rock fracture toughness determination using a semi-circular bend specimen in split Hopkinson pressure bar testing. Rock Mech Rock Eng 49:731–745

Xuan KJ, Zhang YS (2016) Determination of peak and residual strength of jointed rock masses based on GSI system. Site Investig Sci Technol 5:1–6

Yang SQ, Jiang YZ, Xu WY, Chen XQ (2008) Experimental investigation on strength and failure behavior of pre-cracked marble under conventional triaxial compression. Int J Solids Struct 45:4796–4819

Yu XZ, Qiao CX, Zhou QL (1991) Fracture mechanics of rock and concrete. Central South Industrial University Press

Zhang XN, Sheng ZP, Li X, Li SD, He JM (2011) Study of relationship between poisson's ratio and angle of internal friction for rocks. Chin J Rock Mech Eng 30:2599–2609

Zhao YL, Zhang LY, Wang WJ, Pu CZ, Wan W, Tang JZ (2016) Cracking and stress–strain behavior of rock-like material containing two flaws under uniaxial compression. Rock Mech Rock Eng 49:2665–2687

Zhao YL, Zhang LY, Wang WJ, Tang JZ, Lin H, Wan W (2017a) Transient pulse test and morphological analysis of single rock fractures. Int J Rock Mech Min Sci 91:139–154

Zhao YL, Luo SL, Wang YX, Wang WJ, Zhang LY, Wan W (2017b) Numerical analysis of karst water inrush and a criterion for establishing the width of water-resistant rock pillars. Mine Water Environ 36:508–519

Zhao YL, Tang JZ, Chen Y, Zhang LY, Wang WJ, Wan W, Liao JP (2017c) Hydromechanical coupling tests for mechanical and permeability characteristics of fractured limestone in complete stress–strain process. Environ Earth Sci 76:1–18

Zhao YL, Wang YX, Wang WJ, Wan W, Tang JZ (2017d) Modeling of non-linear rheological behavior of hard rock using triaxial rheological experiment. Int J Rock Mech Min Sci 93:66–75

Zhao YL, Zhang LY, Wang WJ, Wan W, Li SQ, Ma WH, Wang YX (2017e) Creep Behavior of intact and cracked limestone under multi-level loading and unloading cycles. Rock Mech Rock Eng 50:1409–1424

Zhao YL, Zhang LY, ASCE M, Wang WJ, Wan W, Ma WH (2018) Separation of elastoviscoplastic strains of rock and a nonlinear creep model. Int J Geomech 18(04017129):1–18

Zhao YL, Wang YX, Wang WJ, Tang LM, Liu Q, Cheng GM (2019) Modeling of rheological fracture behavior of rock cracks subjected to hydraulic pressure and far field stresses. Theor Appl Fract Mech 101:59–66

Zhou JW, Xu WY, Shi C (2007) Investigation on compression-shear fracture criterion of rock based on failure criterion. Chin J Rock Mech Eng 26:1194–1201

Zuo JP, Li HT, Xie HP, Ju Y, Peng SP (2008) A nonlinear strength criterion for rock-like materials based on fracture mechanics. Int J Rock Mech Min Sci 45:594–599